

# Unsupervised Tumour Segmentation in PET Based on Active Surface Modelling and Alpha Matting

Ziming Zeng<sup>1,2</sup>

zzz09@aber.ac.uk

Reyer Zwiggelaar<sup>1</sup>

rrz@aber.ac.uk

<sup>1</sup>Department of Computer Science

Aberystwyth University, Aberystwyth, UK

<sup>2</sup>Faculty of Information and Control Engineering

Shenyang Jianzhu University, Shenyang, China

## Abstract

This paper presents a novel, unsupervised method for segmenting tumours in PET data. The method uses region-based active surface modelling in a hierarchical scheme to eliminate segmentation errors, followed by an alpha matting step to further refine the segmentation. We have validated our method on real PET images of head-and-neck cancer patients as well as custom designed phantom PET images. Experiments show that our method can generate more accurate segmentation than some previous approaches.

## 1 Introduction

Positron emission tomography (PET) is widely used for tumour imaging in cancer diagnosis, staging, treatment evaluation and radiotherapy planning, which require accurate segmentation of the volume of interest (VOI). Segmentation of PET VOIs is commonly performed by a combination of manual delineation and intensity thresholding. Manual segmentation is time-consuming and highly variable. Intensity thresholding lies at the core of most fully- or semi-automatic VOI segmentation methods [9]. More advanced methods include the Poisson Gradient Vector Flow (PGVF) of Hsu et al. [2] and the Markov Random Field Expectation Maximisation (MAP-MRF EM) labelling technique of Gribben et al. [4]. In this paper we propose a new VOI segmentation method for PET, which employs a hierarchical approach combining an improved region-based active surface model and alpha matting.

## 2 Image Segmentation Method

Our hierarchical segmentation scheme consists of three steps. (see Fig. 1). In the first two steps, an improved 3D active surface modelling method is used to segment the VOIs. In the last step, a trimap which contains a definite foreground, a definite background and an unknown region is automatically generated and an alpha matting technique is used to refine the segmentation results.

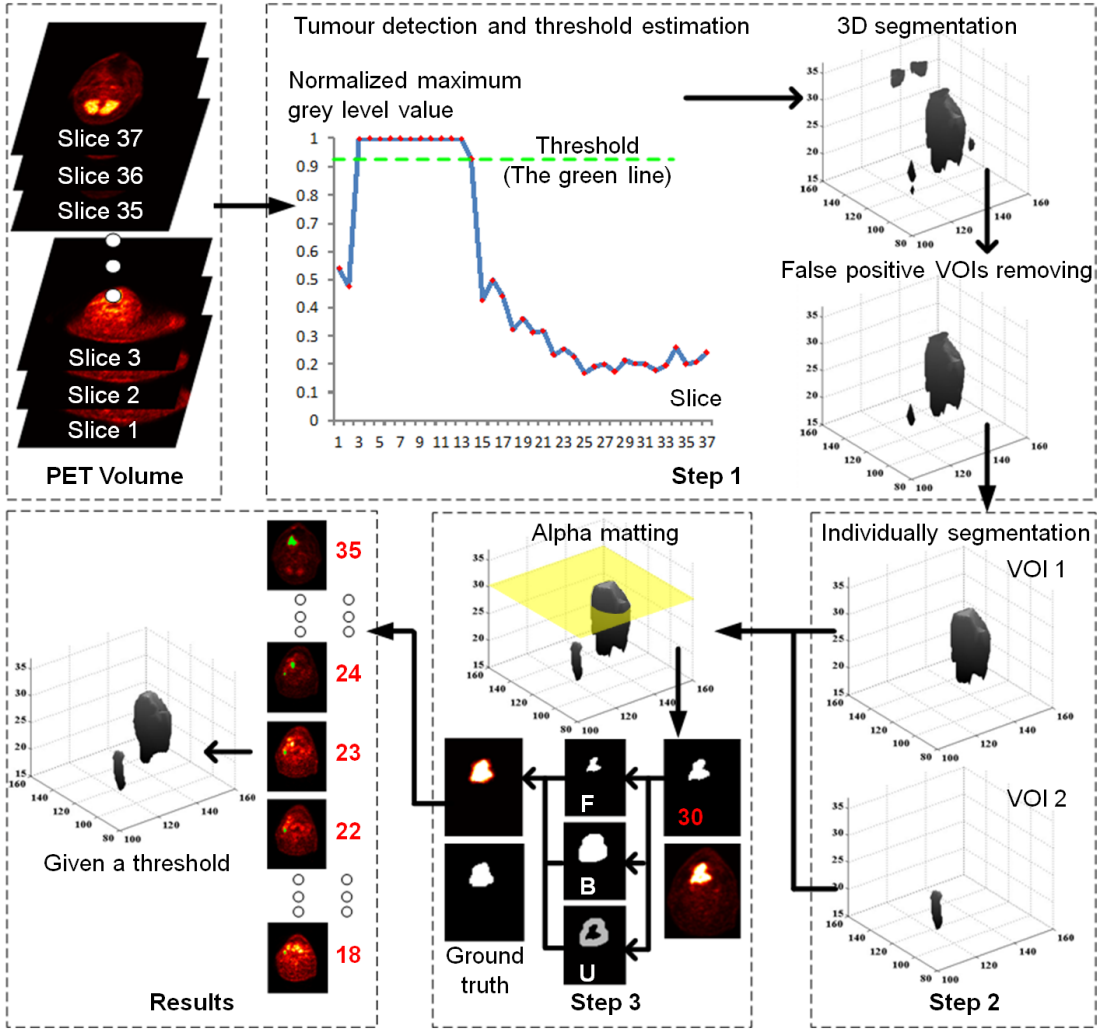


Figure 1: Segmentation results of the hierarchical segmentation approach. The tumour is shown in green on each slice of the original volume. Tumour images are labeled with red color numbers

## 2.1 Improved 3D Active Surface Modelling

A region-based active surface model [3] and a global convex segmentation model [5] are used to obtain an energy functional that can be minimized by convex optimization. Subsequently, the energy functional is minimized along with the deformation of the surface using a Split Bregman technique [6]. As in [10], the energy functional is formally defined as:

$$E = f_1 f_2 \quad x \quad f_1 x \quad f_2 x \quad dx \quad v \quad H \quad x \quad dx \quad P \quad (1)$$

where  $\Gamma$  denotes the surface of tumours,  $P = \frac{1}{2} \int_{\Gamma} |x - v|^2 dx$  is the level set regularization term. In our work, we extend the method in [10] into 3D segmentation. The region-scalable energy functional is defined as

$$x \quad f_1 x \quad f_2 x \quad \sum_i^2 K(x, y) f_i(x) |I(y)|^2 M_i(y) dy \quad (2)$$

where  $K$  is 3D Gaussian kernel functional. Given the locality of the kernel functional, the effect on  $f_i$  generated by  $I(y)$  is almost zero when  $y$  is far away from  $x$ . The local fitting energy  $f_i$  is determined by the value of  $I(y)$ . In Eq. 2,  $M_1 = H - M_2 = 1 - H$ . The Heaviside functional  $H$  is usually approximated by a smooth functional  $H(x) = 1 - e^{-|x|}$

$\frac{2}{\pi} \arctan x$ . As the grey level of tumours can vary between volumes, we change this functional to

$$H(x) = \frac{1}{2} \left( 1 - \frac{2}{\pi} \arctan \left( \frac{x-T}{2} \right) \right) \quad (3)$$

where  $T (0 < T < 1)$  is a normalisation value which is the tumour grey level threshold.

According to the derivation by Li et al. [3], the optimal functionals  $f_1(x), f_2(x)$  which minimize  $E = f_1 + f_2$  are:

$$f_i(x) = \frac{K(x) M_i(x) I(x)}{K(x) M_i(x)} \quad i = 1, 2 \quad (4)$$

For fixed  $f_1(x), f_2(x)$ , the functional  $E$  can be written as:

$$\frac{\partial}{\partial t} \left( \frac{1}{2} e_1^2 + \frac{1}{2} e_2^2 \right) = \operatorname{div} \left( \frac{\partial E}{\partial r} \right) \quad (5)$$

where  $e_i$  is the derivative of  $H \cdot f_i(x) = K(y) x \cdot I(x) - f_i(y)^2 dy$   $i = 1, 2$ . The simplified flow represents the gradient descent for minimizing the energy:

$$\frac{\partial r}{\partial t} = -e_1 - e_2 \quad (6)$$

where  $r = e_1 + e_2$ . Yang et al. [10] restricted the solution to lie in a finite interval in order to transform the constrained optimization problem to an unconstrained one. In this work, we constrain  $r$  as  $0 \leq r \leq 1$ , which can guarantee a unique global minimal. The global convex model can be written as  $\min_0 \frac{1}{2} E^2 + \min_0 \frac{1}{2} (1 - r)^2$ . In [10], the minimization problem was written as  $\min_0 \frac{1}{2} E^2 + \min_0 \frac{1}{2} g(r)$ , where  $g(r) = 1 - r^2$ , is a constant value. Then the Split Bregman method is used to minimize the energy functional [10]. When the optimal  $r$  is found, we can find the segmented region  $k \subset x : |k(x)| \leq 0.5$ .

## 2.2 Hierarchical Segmentation Scheme

As preprocessing, significantly noisy images are discarded before 3D volume data is generated. In the first segmentation step, we extract a closed surface area by using a low threshold as the initial surface to segment the PET volume data. The threshold  $T$  in Eq. 3 is estimated by calculating the average of the maximum grey level values of some selected slices in the volume. Specifically, we find the maximum grey level value for each slice. then all the values are normalized between 0 to 1. Subsequently, we select the slice which contains the maximum value. This slice will be utilised to compare with its three left neighbouring slices (named left neighbouring window). If the difference between this slice and any of the slice in the left window is less than the threshold  $\epsilon$ , move the current slice to its closest left slice and compare the slice with its corresponding left window. This propagation carries on until the difference is above the threshold  $\epsilon$ . The selected slices are propagated in this way. The same process is also imposed to the right side. Finally, we calculate the average of the maximum value from all the selected slices as the threshold  $T$ . For robust segmentation, a reliability metric is used to remove false positive VOIs. Specifically, the 6-connected neighborhood voxels are labeled in the results. If the tumour only exists in one or two slices, then the corresponding 3D labelling will be removed from the results.

The second segmentation step tries to find the non-detected regions that are selected in the first step. Specifically, morphology is used to dilate each 3D VOI generated in the previous step. We then use the generated surface as the initial closed surface, and segment the VOIs again using the local grey level voxels. The threshold  $T$  in this step is estimated by computing the average grey level values of the voxels in each dilated VOI.

## 2.3 Segmentation by Using Alpha Matting

Due to the partial volume effect and limited image resolution, the segmentation results generated by the first two steps are not accurate enough. To further improve the segmentation accuracy, we introduce an alpha matting method [1] into our segmentation pipeline. Instead of generating binary segmentation labels, an alpha matting techniques can generate a fractional alpha values between 0 and 1 for these pixels, which can be viewed as accurate soft segmentation.

To use alpha matting, a trimap has to be generated at first, which separates the image into three regions: definite foreground  $F$ , definite background  $B$ , and the unknown region  $U$ . Our system automatically generates this trimap. Specifically, we use morphology to erode the previous segmentation result with a circular structuring element to obtain the foreground  $F$ , then the background  $B$  can be generated by dilating the binary segmentation. The unknown area can be generated by using the combined results. To solve the alpha matting problem, we use the approach proposed by Levin et al. [1]. Solving the matting problem leads to a soft segmentation of VOIs in PET images.

## 3 Experiment

To evaluate our method, we use 2 PET images of head-and-neck cancer patients and 2 of a custom-built tumour phantom [7, 8]. All images were acquired using a hybrid PET/CT scanner (GE Discovery) and the metabolic tracer [ $^{18}\text{F}$ ]FDG. Ground truth was derived for each phantom VOI by thresholding the CT images and for each patient tumour by manual delineation.

The detailed segmentation process for the example of a patient tumour is shown in Fig. 1. The clinical data sets are 256 256 37 voxels. In the first step, all the maximum grey level values are generated from the 37 slices in the volume. Subsequently, the selected slices from 2 to 15 are identified by using the proposed criteria ( $\sigma = 0.12$ ), then the threshold  $T$  in Eq. 3 is automatically estimated as 0.916. In Eq. 2, the 3D Gaussian kernel  $\sigma$  is 3 and  $\sigma_i = 10$ . In Eq. 3,  $\sigma = 0.1$ . The improved active surface modelling result is used to segment the image and four false positive labellings are automatically removed. In the second step, the threshold  $T$  is recalculated for each dilated VOI and two VOIs are segmented again. We can see some non-detected regions are identified in this step. In the third step, the alpha matting algorithm is used to refine the segmentation on each slice. To compare against the ground truth which is a binary image, we threshold the soft segmentation generated by matting at half of the maximum grey level value for each slice, which leads to the final binary segmentation of VOIs.

Fig. 2 shows a comparison with other methods on real and phantom PET data. Over-segmentation in the red region of the original image is apparent for the PGVF and MAP-MRF EM methods. This is partly explained by partial volume effects and the low spatial resolution of the images but could also be due to these slice-wise methods ignoring volumetric grey

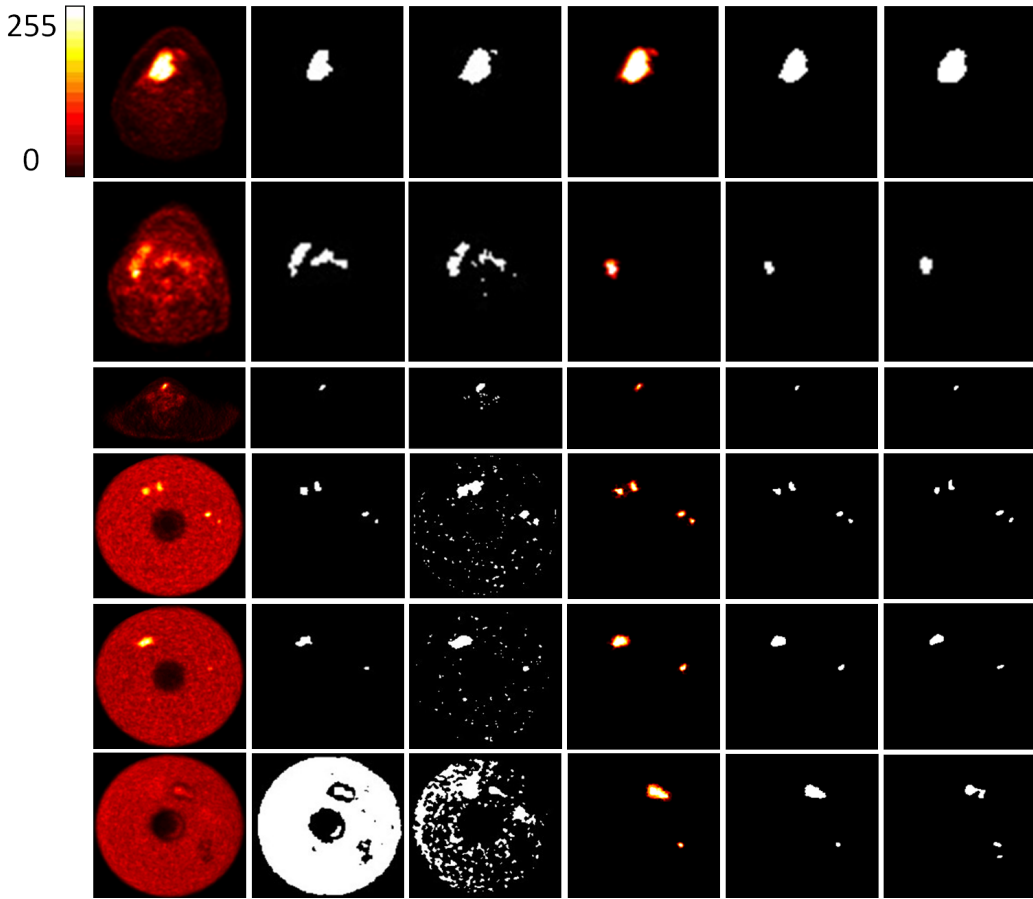


Figure 2: Segmentation of the patient VOIs. From left to right: Color bar shown from 0 to 255, PET data (patient data (slice 28, slice 21 in patient A, and slice 9 in patient B), phantom data (slice 22, slice 26 in phantom C, and slice 21 in phantom D)), PGVF, MAP-MRF EM, our method, our results after half threshold, ground truth.

level information. For the phantom data, the MAP-MRF EM method does not perform well on images with significant noise. The PGVF method fails to segment the abnormal region, because the density of the abnormal region is similar to the surrounding tissue. In contrast, the developed method performs well with these images and provides accurate segmentation results.

We evaluate segmentation accuracy in terms of overlap with ground-truth using the Dice similarity coefficient (DSC). We compare the DSC of our method and alternative approaches [2, 4]. Tab. 1 shows the mean DSC for real and phantom PET as well as the overall mean. Our results show improvements compared to previous methods.

## 4 Discussion and Conclusions

This paper presents a novel PET image segmentation scheme, based on an improved region-based active surface modelling method and alpha matting. Our method has the following advantages. First, the 3D voxel information is considered in a hierarchical scheme, which can largely eliminate segmentation errors. Second, the alpha matting technique is introduced to PET image segmentation for the first time, which can effectively deal with the partial volume effect problem. Finally, compared with previous approaches, our method is more robust on PET imaging segmentation. As future work, we will further evaluate our method

Table 1: Dice index for tumour segmentation on PET data

Algorithm	PGVF [2]	MRF [4]	Our method (half thresholding results)
Patient images	0.562	0.430	0.706
Phantom images	0.423	0.383	0.664
All images	0.493	0.407	0.685
Standard deviations	0.234	0.218	0.142

on larger clinical datasets.

## References

- [1] A.Levin, D.Lischinski, and Y.Weiss. A closed form solution to natural image matting. *IEEE Trans. Pattern Analysis and Machine Intelligence*, 30:228-242, 2008.
- [2] C.Hsu, C.Liu, and C.Chen. Automatic segmentation of liver PET images. *Computerized Medical Imaging and Graphics*, 32:601-610, 2008.
- [3] C.Li, C.Kao, C.John, and Z.Ding. Minimization of Region-Scalable Fitting Energy for Image Segmentation. *IEEE Trans. Image Processing*, 17, 1940-1949, 2008.
- [4] H.Gribben, P.Miller, H.Wang, K.Carson, A.Hounsell, and A.Zatari. Automated MAP-MRF EM labelling for volume determination in PET. *ISBI*, 1-4, 2008.
- [5] T.F.Chan, S.Esedoglu, and M.Nikolova. Algorithms for finding global minimizers of denoising and segmentation models. *SIAM Journal on Applied Mathematics*, 66:1632-1648, 2006.
- [6] T.Goldstein, X.Bresson, and S.Osher. Geometric Applications of the Split Bregman Method: Segmentation and Surface Reconstruction. *Journal of Scientific Computing*, 45:272-293, 2010.
- [7] T.Shepherd, M.Teräs, and H.Sipilä. New Physical Tumour Phantom and Data Analysis Technique Exploiting Hybrid Imaging and Partial Volume Effects for Segmentation Evaluation in Radiation Oncology. *European Journal of Nuclear Medicine and Molecular Imaging*, 37:S221, 2011.
- [8] T.Shepherd, M.Teräs, and H.Sipilä. Results of the Contouring Challenge, Software Session II at the XII Turku PET Symposium, Turku PET Centre, Finland. [*online*]. Available: [http://www.turkupetcentre.net/PET\\_symposium\\_XII\\_software\\_session/ContouringChallengeResults/](http://www.turkupetcentre.net/PET_symposium_XII_software_session/ContouringChallengeResults/), 2011.
- [9] Y.E.Erdi, O.Mawlawi, S.M.Larson, M.Imbriaco, H.Yeung, R.Finn, and J.L.Humm. Segmentation of lung lesion volume by adaptive positrone mission tomography image thresholding. *Cancer*, 80:2505-2509, 1997.
- [10] Y.Yang, C.Li, C.Kao, and S.Osher. Split Bregman method for minimization of region-scalable fitting energy for image segmentation. *Lecture Notes in Computer Science*, 6454, 117-128, 2010.